Chinese Journal of Chemistry, **2004**, *22*, 1250—1256 **Article**

XPS Characterization of Carbon Nanotube Supported CoMo Hydrodesulfurization Catalysts

SHANG, Hong-Yan*,[a](商红岩) LIU, Chen-Guang[a](刘晨光) ZHAO, Rui-Yu[a](赵瑞玉)
WU, Ming-Bo[b](吴明铂) WEI, Fei[c](魏飞)

[a] *Key Laboratory of Catalysis, Chinese National Petroleum Corporation (CNPC), University of Petroleum, Dongying, Shandong 257061, China*
[b] *State Key Laboratory of Heavy Oil Processing, University of Petroleum, Dongying, Shandong 257061, China*
[c] *Department of Chemical Engineering, Tsinghua University, Beijing 100084, China*

In this paper, the effect of catalytic support and sulfiding method on the chemical state of supported Co-Mo catalysts is studied by XPS. After sulfidation with *in-situ* method, the majority of molybdenum in CNT supported CoMo catalyst is transferred to a species with a formal chemical state Mo(IV) in MoS_2 phase, and the rest to Mo(V) which consists of Mo coordinated both to O and S, such as $MoO_2S_2^{2-}$ and MoO_3S^{2-}. In case of CoMo/γ-Al_2O_3 catalyst sulfided with *in-situ* method, a fraction of molybdenum is transferred to formal state Mo(IV) in the form of MoS_2, but there is still a mount of unreduced Mo(VI) phase which is difficult to be sulfided. In CoMo/CNT catalytic system sulfided with *ex-situ* method, Mo(IV) in the form of MoS_2 is detected along with a portion of unreduced Mo(VI) phase, suggesting that not all the Mo phases are reduced and sulfided by *ex-situ* method. As for CoMo/γ-Al_2O_3, a portion of molybdenum is sulfided to intermediate reduced state Mo(V) which consists of Mo coordinated both to O and S, such as $MoO_2S_2^{2-}$ and MoO_3S^{2-}, in addition, there is still a fraction of unreduced Mo(VI) phase. XPS analyses results suggest that CNT support facilitates the reduction and sulfidation of active species to a large extent, and that alumina support strongly interacts with active species, hereby producing a fraction of phase which resists complete sulfiding. Catalytic measurements of catalysts in the HDS of dibenzothiophene (DBT) show that CoMo/CNT catalysts are of higher HDS activity and selectivity than CoMo/γ-Al_2O_3 catalyst, which is in good relation with the sulfiding behavior of the corresponding catalyst.

Keywords carbon nanotube, XPS, HDS, molybdenum, Co-Mo catalyst

Introduction

The removal of sulfur, nitrogen and oxygen from petroleum fractions is very important for solving current environmental problems because of the enactment of strict legislation. For this purpose, more active hydrodesulfurization (HDS) catalysts are requested. It is well known that the catalytic performance of Co-Mo HDS catalysts depends on the support used to a certain extent, since the surface properties vary with the changes of the support.[1] Although many efforts have been devoted to alumina supported molybdenum based catalytic systems, considerable studies are also carried out on other supports such as silica,[2] titania,[3] zirconia,[4] mixed oxides[5] and carbon.[6] It is considered that the support affects the reducibility of oxidic species, and modifies the edge dispersion and stacking degree of MoS_2 particles, the local structure and electronic properties of a CoMoS phase. Recently, carbon supported catalyst systems have attracted more and more attention.[7] Carbon supported hydro-treating catalysts possess very good properties in many aspects, such as higher activity and a lower coking propensity than classical alumina supported catalytic system.[8] It is known that weak interaction between active species and support such as silica support will lead to a decreasing of dispersion, and that very strong chemical interaction between active phases and support such as alumina will improve the dispersion of active species, but will form a portion of active phases which are hard to be reduced into low electronic state during sulfiding step. The extent of sulfidation of the active phases is determined by the structure of the oxidic precursor species, which is dependent on the support used to a certain extent.[9]

In this paper, we attempted to investigate the effect of carbon nanotube support on the chemical state and reducibility of supported oxidic precursor Co-Mo catalysts by X-ray photoelectron spectroscopy (XPS) and temperature-programmed reduction (TPR) technique. The influence of sulfiding method on the sulfidation extent of active species was also studied by XPS. The aim of the present work was to compare the supports

* E-mail: catagroupsh@hotmail.com; Tel./Fax: +86-546-839-2284
Received November 19, 2003; revised April 20, 2004; accepted July 10, 2004.
Project supported by the Foundation of Chinese National Petroleum Corporation for a Basic Research (No. 03A5050101).

and sulfiding method in relation to the catalytic performance in the HDS of dibenzothiophene (DBT).

Experimental

Catalyst preparation

A kind of multiwalled carbon nanotube (CNT) supplied by Tsinghua University was used as-received (BET surface area 189 m^2/g, average pore diameter 8.9 nm, pore volume 0.43 cm^3/g). The catalysts were prepared by pore volume impregnation using aqueous solutions of $(NH_4)_6Mo_7O_{24}\cdot 24H_2O$ and $Co(NO_3)_2\cdot 6H_2O$ (both A.R.). The Mo phase (calculated 10 wt% MoO_3) was introduced first and dried in air at 110 ℃ for 12 h, then Co precursor was introduced with pore volume impregnation followed by drying at 110 ℃ for 12 h again, and finally the bimetallic catalysts were heat-treated at 500 ℃ for 2 h in a flow of nitrogen. Catalysts with Co/Mo atomic ratio of 0.35 and 0.7 were obtained in this way. The oxide state catalyst was labeled CoMo-0.35/CNT and CoMo-0.7/CTN, respectively, where 0.35 and 0.7 represented Co/Mo atomic ratio.

In the preparation of sulfide state Co-Mo catalysts, two methods were used. Sulfiding method I was related to the so-called *in-situ* sulfidation. The samples were sulfided in a flow of 5% H_2S in H_2 at a flow rate of 40 cm^3/min under atmospheric pressure for 6 h, and the temperature was kept at 400 ℃ during the sulfiding process. After sulfidation, the samples were cooled to room temperature under a flow of high purity argon, and put into desiccator under the protection of argon as soon as possible. The sulfide sample was labeled as S-CoMo/CNT and S-CoMo/γ-Al_2O_3, respectively. Sulfiding method II was related to the so-called *ex-situ* pre-sulfidation. Sulfide Mo phase was provided by ammonium tetrathiomolybdate (ATTM)[10] followed by the impregnation of $Co(NO_3)_2\cdot 6H_2O$ and dried at 110 ℃ for 24 h, and finally heat-treated at 500 ℃ in a flow of N_2 for 4 h. The sulfide catalysts were labeled as CoMoS/ CNT and CoMoS/γ-Al_2O_3, respectively.

Temperature-programmed reduction (TPR)

TPR measurements were performed using a self-installed TPD-TPR apparatus. 0.1 g of sample was placed into a U shaped stainless steel reactor filled with quartz. The sample was flushed with high purity nitrogen at 300 ℃ for 1 h and cooled down to 50 ℃. After treatment with nitrogen, a flow of mixed 6 vol.% H_2/N_2 gas was inducted into the system at a rate of 30 mL/min at 50 ℃ until a high quality base line was obtained. Finally, the sample was heated from 50 to 800 ℃ at a rate of 8 ℃/min under a very steady flow of mixed 6 vol.% H_2/N_2 gas monitored by two flow meter controllers. During the operation, the exit gases from the reactor passed through a cold trap filled with ice and salt in order to remove the water from the exit steam. Consumption of H_2 was monitored by thermal conductivity detector (TCD). The TPR profiles were analyzed using professional software.

XPS analysis

The X-ray photoelectron spectroscopy (XPS) analyses were performed on a PHI 5300X instrument, equipped with a dual Mg/Al anode. The spectra were exited by the Mg Kα source (1235.86 eV) run at 12.5 kV and 150 mA. The analyzer operated in the constant analyzer energy (CAE) mode. For individual peak energy regions, a pass energy of 20 eV set cross the hemisphere was used. Survey spectra were measured at 50 eV pass energy. The sample powders were analyzed as pellets, mounted on a double sided adhesive tape. The pressure in the analysis chamber was in the range of 1.33×10^{-6}—1.33×10^{-7} Pa during the data collection. The constant charging of the samples was removed by referencing all the energies to the C1s set at 285.0 eV, arising from the adventitious carbon. Analyses of the peaks (fitting, integration and background subtract) were performed with the software Apollo Series 3500. The binding energy (BE) values were estimated to be accurate within $\pm$0.2 eV. The spin-orbit spitting of Mo3d peaks was 3.1 eV. The $Mo3d_{5/2}/Mo3d_{3/2}$ area ratios were kept constant and equal to the theoretical value of 1.5.

HDS measurements

The HDS catalytic activity tests were performed in a high pressure continuous flow micro-reactor system operating at 280 ℃, p_{H_2}=2 MPa, $LHSV$=6 h^{-1}. Prior to the HDS test, the catalyst was sulfided at 400 ℃ and 2 MPa of H_2 for 4 h, using a mixture of 3 mol% CS_2 in cyclohexane as liquid feed.

Results and discussion

TPR

The TPR curves of oxidic Co-Mo/CNT and Co-Mo/γ-Al_2O_3 catalysts are given in Figure 1. As for CoMo-0.35/CNT, there are only two reduction processes, the low temperature reduction mainly occurs at 481 ℃, and the peak at 659 ℃ corresponds to the active species which is relatively difficult to be reduced. There are three hydrogen consumption peaks in TPR curve of CoMo-0.7/CNT corresponding to three reduction processes, the first one is located at 260 ℃ in low temperature region with a small shoulder peak on the right (about 362 ℃), and the last weak peak appears at 740 ℃ in high temperature region. In case of Co-Mo/γ-Al_2O_3, the reduction of well-dispersed MoO_3 species is at about 791 ℃ and the reduction of bulk MoO_3 is located at about 490 ℃, which is consistent with the result in Ref. 11. The TPR results reveal that the active species on Co-Mo/CNT are more easily reduced than those in Co-Mo/γ-Al_2O_3, indicating that the CNT support favors the reduction of active species. It also shows that Co/Mo atomic ratio has great influence on the number of active species existing in the catalysts and on the reducibility of active phases.

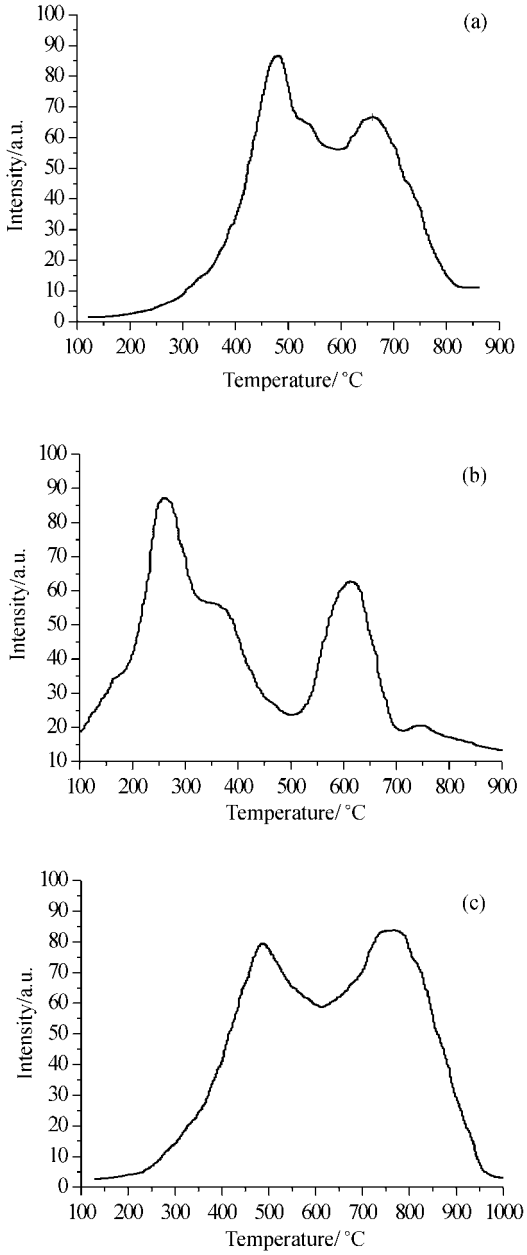

Figure 1 TPR curves of oxidic catalysts. (a) CoMo-0.35/CNT, (b) CoMo-0.7/CNT and (c) CoMo-0.35/γ-Al_2O_3.

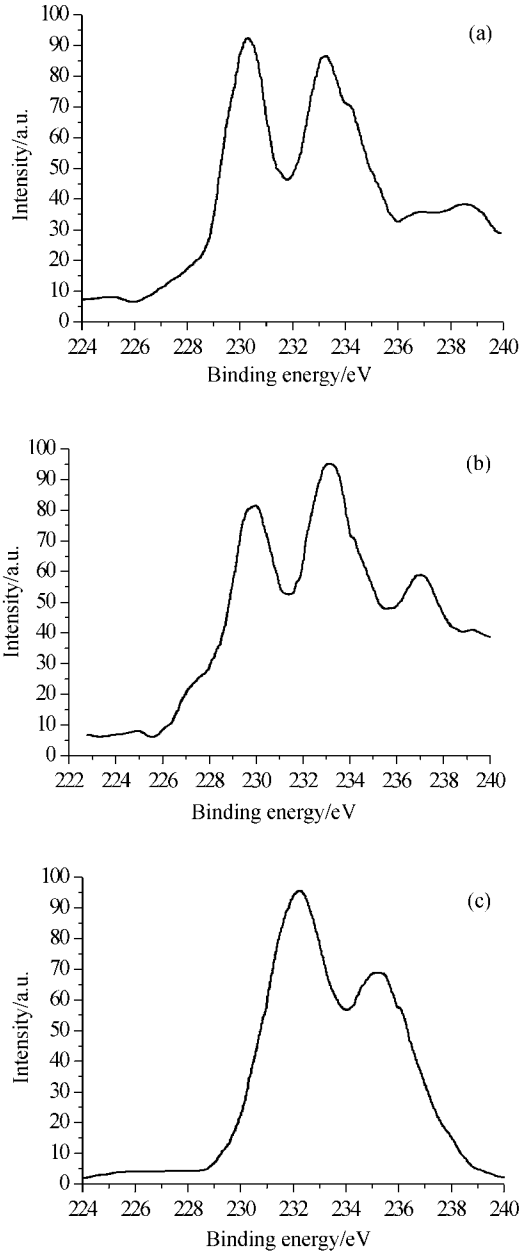

Figure 2 Mo3d spectra of oxidic samples. (a) CoMo-0.35/CNT, (b) CoMo-0.7/CNT and (c) CoMo-0.35/γ-Al_2O_3.

XPS

Figure 2 presents the Mo3d spectra of oxidic samples. The binding energies (BE), full width at half maximum (FWHM), the bind energy difference (ΔE) between the Co2p and S2p levels, the surface atomic concentrations and surface atomic ratios are given in Table 1 and Table 2, respectively. As for carbon nanotube supported oxidic CoMo catalyst with Co/Mo atomic ratio 0.35 (Figure 2a), the doublet with the Mo $3d_{5/2}$ peak at about 228.68 eV is typical of Mo(IV) in oxidic forms.[12] The additional doublet with main $Mo3d_{5/2}$ peak at around 231.16 is attributed to the intermediate reduced state Mo(V). Similarly, in the sample of CoMo-0.7/CNT (Figure 2b), the doublet with the $Mo3d_{5/2}$ peak at about 228.86 eV is the contribution of Mo(IV) in oxidic forms and the additional doublet with main $Mo3d_{5/2}$ peak at around 231.16 eV is attributed to the intermediate reduced state Mo(V). But unlike CoMo-0.35/CNT, a fraction of unreduced Mo(VI) component (about 30.6 wt%) is still found at 232.0 eV. In case of oxidic Co-Mo/γ-Al_2O_3 catalyst (Figure 2c), the binding energies of the $Mo3d_{5/2}$ (232.1 eV) and $Mo3d_{3/2}$ (235.2 eV) photoelectrons, as well as the BE difference of the two peaks, are characteristic of Mo(VI) supported species in an oxidic surroundings. Taking the FWHM values into account, the relatively lower FWHM values of carbon nanotube supported oxidic Co-Mo catalysts compared with those of CoMo/γ-Al_2O_3 indicate that the interaction of active species with carbon nanotube is weaker than that with alumina, in other word, the interaction between active phases and alumina support is stronger. In addition, the surface atomic

Table 1 M3d, Co2p, S2p binding energies (eV) and full width at half maximum (FWHM)

Catalyst	Binding energy[b]/eV				ΔE(Co2p$_{3/2}$-S2p)/eV	FWHM[d]/eV
	Mo3d$_{5/2}$	Mo3d$_{3/2}$	Co2p	S2p		
CoMo/CNT(0.35)[a]	228.68 (46.9)[c] 231.16 (53.1)	231.8 234.71	778	—	—	1.6
CoMo/CNT(0.7)	228.86 (22.1) 231.36 (47.3) 232.0 (30.6)	232.04 234.4 235.1	781.5	—	—	1.7
CoMo/γ-Al$_2$O$_3$(0.35)	232.1	235.2	780.1	—	—	1.8
S-CoMo/CNT(0.35)	227.96 (60.18) 231.04 (39.82)	231.16 234.25	778.5	161.19 (2.4)[e] 163.25 (2.7) 167.87 (3.0)	616.7	1.8
S-CoMo/CNT(0.7)	227.84 (47.1) 230.88 (52.9)	231.7 234.93	779	161.0 (1.9) 162.95 (2.5) 167.87 (2.6)	618	1.6
S-CoMo/γ-Al$_2$O$_3$ (0.7)	228.6 (58.2) 232.0 (41.8)	231.5 235.1	778.6	162.6 (3.0) 168.1 (3.2)	616	1.9
CoMoS/γ-Al$_2$O$_3$(0.7)	230.54 (28.93) 232.76 (49.5)	233.6 235.66	779	162.1 (2.3) 168.2 (3.2)	616.9	1.9
CoMoS/CNT(0.7)	227.56 (47.5) 232.06 (53.5)	230.56 235.56	779	154.15 (3.2) 161.68 (3.8) 167.71 (3.2)	624.85	1.7

[a] Calculated Co/Mo atomic ratio in the preparation of catalyst. [b] Referred to the 1s level at 285.0 eV of adventitious carbon. [c] Percentage of different species resulting from the curve fitting analysis. [d] Full width at half maximum of peak Mo3d$_{5/2}$. [e] Full width at half maximum of peak S2p.

Table 2 Surface atomic concentration and atomic ratio

Catalyst	Surface atomic concentration/%				Atomic ratio		
	Mo	Co	O	S	S/Co+Mo	S/Mo	Co/Mo
CoMo/CNT(0.35)	0.23	0.06	13.6	—	—	—	0.26
CoMo/CNT(0.7)	0.3	0.08	15.7	—	—	—	0.266
CoMo/γ-Al$_2$O$_3$(0.35)	6.77	2.99	18.5	—	—	—	0.44
S-CoMo/CNT(0.35)	0.41	0.16	7.91	1.81	3.17	4.14	0.39
S-CoMo/CNT(0.7)	0.54	0.22	9.99	2.05	2.69	3.79	0.407
S-CoMo/γ-Al$_2$O$_3$(0.7)	2.48	1.43	8.72	1.89	0.48	0.76	0.57
CoMoS/γ-Al$_2$O$_3$(0.7)	1.45	1.11	3.1	1.08	0.42	0.774	0.76
CoMoS/CNT(0.7)	0.44	0.13	2.0	2.67	4.68	6.06	0.295

Desulfurization ratio %=amount of (BPN+CHB)/total amount of DBT; selectivity=amount of BPN /amount of CHB; T=280 ℃, p_{H_2}=2 Mpa, $LHSV$=6 h^{-1}.

concentrations of Co and Mo on Co-Mo/γ-Al$_2$O$_3$ are much higher than those on Co-Mo/CNT catalyst, respectively.

The experimental and fitted X-ray photoelectron spectra of the Mo3d level for catalysts sulfided with method I are shown in Figure 3. The majority of molybdenum in carbon nanotube supported CoMo catalyst is transferred to a species with a binding energy of Mo3d$_{5/2}$ 227.84—227.96 eV, which may be a combination of the typical binding energy for molybdenum with a formal chemical state Mo(IV) in MoS_2 phase (stoichiometric or not)[13] and even lower chemical molybdenum state such as Mo(II). The doublet with the Mo3d$_{5/2}$ peak at about 230.88—231.04 eV is typical of Mo(V) which consists of Mo coordinated both to O and S, such as $MoO_2S_2^{2-}$ and MoO_3S^{2-} [14] in S-CoMo/CNT catalysts. Characteristic peak of supported Mo(VI) species with Mo3d$_{5/2}$ binding energy at 232.0 eV is not found,

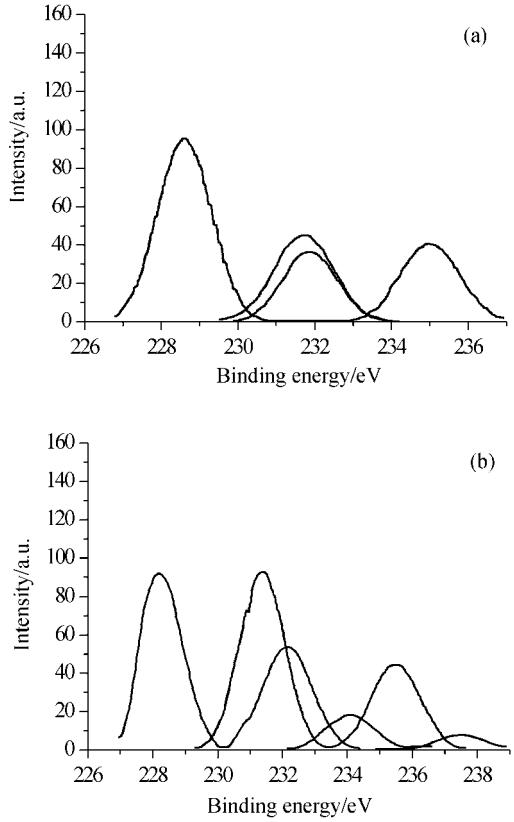

Figure 3 Mo3d XPS spectra of samples sulfided with method I (a) S-CoMo-0.35/CNT and (b) S-CoMo-0.7/CNT.

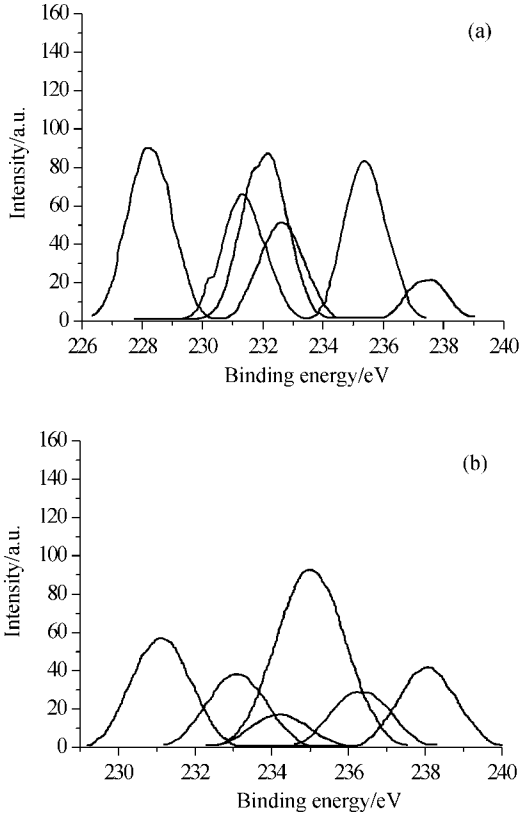

Figure 4 Mo3d spectra of Co-Mo catalysts sulfided with method II (a) CoMoS-0.7/CNT and (b) CoMoS-0.7/γ-Al_2O_3.

indicating that all the Mo species are reduced to Mo(IV) and/or Mo(V) during the sulfiding of CoMo/CNT catalysts with sulfiding method I. The XPS results show that carbon nanotube support facilitates the reduction and sulfidation of active species in CoMo/CNT catalytic system. In case of sulfide CoMoS/γ-Al_2O_3 catalyst which is also sulfided by method I, the doublet with the $Mo3d_{5/2}$ peak at about 228.6 eV is the typical binding energy for molybdenum with a formal state Mo(IV) in the form of MoS_2. In addition, there is still an amount of unreduced Mo(VI) phase left as indicated by the main doublet $Mo3d_{5/2}$ peak at about 232.0 eV, suggesting that there is some kind of Mo phase on the surface of CoMo/γ-Al_2O_3 which is difficult to be reduced and sulfided as a result of strong interaction between alumina support and active species.

Figure 4 compares the Mo3d XPS spectra for Co-Mo/CNT and Co-Mo/γ-Al_2O_3 sulfided with method II. The $Mo3d_{5/2}$ binding energy at 227.56 eV detected for CoMoS/CNT (Figure 4a) is attributed to Mo(IV) in the form of MoS_2 (or a combination of Mo(II) and Mo(IV) due to the obvious decrease of binding energy at 227.56 eV compared with the typical binding energy of Mo(IV) at (229.1$\pm$0.2) eV). There is still a portion of unreduced Mo(VI) phase as evidenced by the existence of $Mo3d_{5/2}$ peak at 232.0 eV, which is the typical binding energy of Mo(VI), suggesting that not all the Mo phases are reduced and sulfided during sulfiding by method II as a result of the absence of H_2 atmosphere. In the XPS spectrum of Mo3d of CoMoS/γ-Al_2O_3 (Figure 4b), binding energy of $Mo3d_{5/2}$ at 230.54 eV is typical of Mo(V) which consists of Mo coordinated both to O and S, such as $MoO_2S_2^{2-}$ and MoO_3S^{2-} (O atoms origin from the Co precursor). Similarly, there is still a fraction of unreduced Mo(VI) phase consisting of a Mo3d doublet with a $Mo3d_{5/2}$ binding energy of 232.0 eV.

The presence of sulfur in samples after sulfidation with method I is confirmed by the peaks of S2p consisting of two peaks after fitting at 161.19 and 163.25 eV for S-CoMo-0.35/CNT (Figure 5a), 161.19 and 162.95 eV (Figure 5b) for S-CoMo-0.7/CNT, respectively. The XPS binding energy at around (161.0$\pm$0.2) eV can be assigned to terminal S_2^{2-} and/or S^{2-} ligands present in MoS_2.[15] The binding energy at (163.0$\pm$0.2) eV is also characteristic of bridging S_2^{2-}, or S^{2-} ligands.[16] The XPS spectra indicate that a considerable fraction of the sulfur in the catalyst sulfided by method I is the S^{2-} ligands present at Mo(IV) in MoS_2. Traces of sulfate species at BE of 167. 87 eV are found in both of the two samples. According to the literature data,[17] the water produced during the sulfiding can cause the oxidation of molybdenum disulfide phase to sulfates. In addition, re-oxidation of sulfide ions during storage and/or XPS analysis could form the sulfates.

Figure 6 compares the XPS spectra of S2p level for sulfide samples sulfided by method II. As for CoMoS-0.7/CNT, binding energy at 161.68 eV is characteristic of bridging S^{2-} and/or S_2^{2-} ligands (Figure 6a).

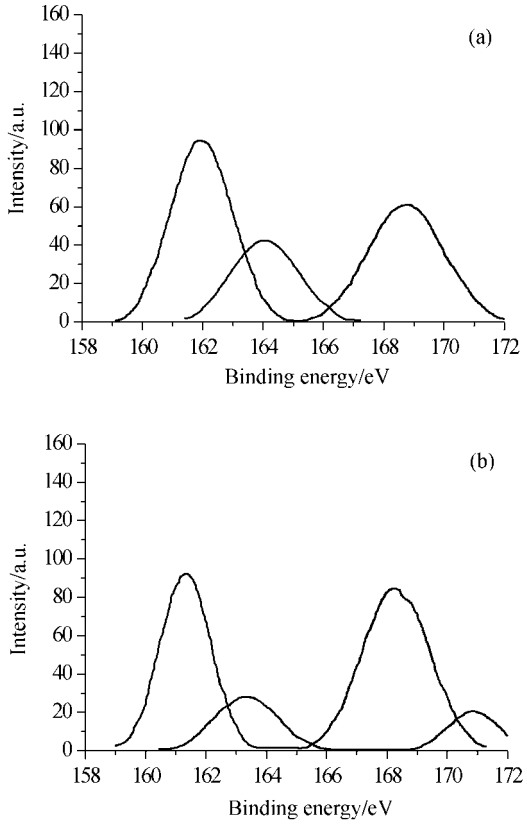

Figure 5 S2p XPS spectra of sulfide samples (a) CoMoS-0.35/CNT and (b) S-CoMo-0.7/CNT.

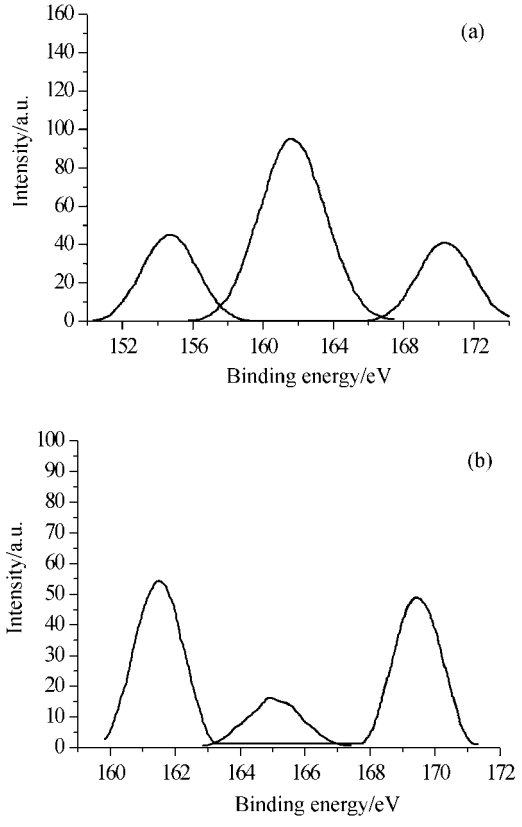

Figure 6 S2p XPS spectra of samples sulfided with method II (a) CoMo-0.7/CNT and (b) CoMo-0.7/γ-Al_2O_3.

Additional 2s peak with binding energy at 154.15 eV is uncertain to which chemical state it is ascribed. Traces of sulfate species at BE of 167. 87 eV are also detected. It is also the case with CoMoS-0.7/γ-Al_2O_3 except the absence of S2p peak with binding energy at (154.15$\pm$0.2) eV. A comparative study of the S/Co+Mo atomic ratio and S/Mo atomic ratio, between alumina supported sulfide CoMo catalyst and carbon nanotube supported Co-Mo catalysts, reveals that the surface S atomic concentration, S/Co+Mo atomic ratio on carbon supported catalyst is much higher than that on the surface of alumina supported catalyst, respectively. This strongly indicates that the active species in CoMo/CNT are more easily sulfided than those in CoMo/γ-Al_2O_3. The changes of Co2p BEs observed among the samples can not be considered significant on the basis of the poor signal to noise ratio.

HDS measurements

In the distribution of products, BPN denotes biphenyl, CHB denotes cyclohexylbenzene, and 4H-DBT represents tetrahydrodibenzothiophene, and DBT represents dibenzothiophene. In order to deal with the experimental data, conversion ratio (wt%) represents total amount of DBT subtracts un-reacted amount of DBT/total amount of DBT, and selectivity is defined as amount of BPN/amount of BPN pluses amount of CHB.

Figure 7 presents the results of HDS activity and selectivity measurements over catalysts. Figure 8 shows the product distributions of HDS reaction of DBT over different catalysts. Accordingly, the CNT supported Co-Mo catalysts are more active than Co-Mo/γ-Al_2O_3 catalyst in the HDS of dibenzothiophene (DBT). All the Co-Mo/CNT catalysts are of high activity (DBT conversion ratio) even at low reaction temperature (280 ℃), and with very high selectivity (hydrogenolysis products/hydrogenation products). The reason for this may be that the surface property of CNT is quite different from that of alumina, such as the weak interaction between active phases and CNT, resulting in the great differences of dispersion, surface atomic concentration of Co, Mo, and S, and the chemical environment of Mo atoms compared with γ-Al_2O_3 catalyst. By contrast, CoMo/γ-Al_2O_3 catalyst shows low activity and low selectivity, producing relatively large amount of hydrogenation product, CHB (15 wt%). It is in good agreement with TPR results and in good relation with the sulfiding behavior of corresponding catalyst. In addition, Co/Mo atomic ratio has great influence on both the HDS activity and the selectivity, and CoMo-0.7/CNT catalyst is the most active one (DBT conversion ratio 100%), while CoMo-0.35/CNT catalyst shows the highest selectivity (BPN 91.18 wt%, CHB 5.53 wt%). The role of Co atoms is still under debate, however, it is generally accepted that the Co atoms promote the activity of Mo through electron transfer with consequently lowering the oxidic state of Mo,[18] and the Co atoms also perturb the local electronic environment of neighboring S atoms involved in the adsorption step of sulfur compounds.[19] It

is believed that the Co atoms are located at the MoS_2 crystallite edges forming the so-called CoMoS structure which is considered to be the active phase in the HDS reaction.[20] In this respect, Co atoms play an important role in affecting the chemical environment of Mo atoms and CoMoS active phase structure via Co/Mo atomic ratio.

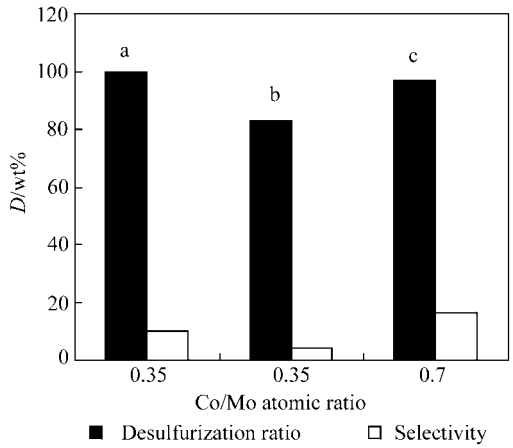

Figure 7 Activity and selectivity of CoMo catalysts (a) CoMo-0.35/CNT, (b) CoMo-0.35/γ-Al_2O_3 and (c) CoMo-0.7/CNT.

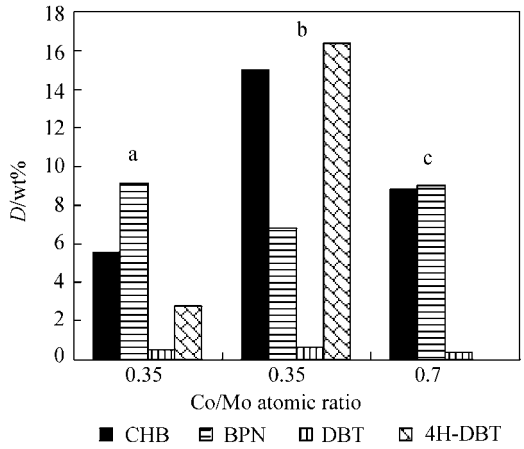

Figure 8 Product distributions of HDS reaction of DBT (a) CoMo-0.35/CNT, (b) CoMo-0.35/γ-Al_2O_3 and (c) CoMo-0.7/CNT.

Conclusions

Based on the XPS analyses, it is concluded that Mo(IV), intermediate reduced state Mo(V) and unreduced Mo(VI) molybdenum phases co-exist on the surface of oxidic CoMo/CNT catalyst. Whereas, there is only one chemical state, unreduced Mo(VI) phase, on the surface of CoMo/γ-Al_2O_3 catalyst.

On the basis of XPS and TPR analyses it is suggested that carbon nanotube support facilitates the sulfidation of active species to a large extent, and alumina support strongly interacts with active species resulting in a fraction of phase which resists complete sulfiding.

As for sulfiding method, it is concluded that sulfiding method I results in complete reduction and partial sulfidation of molybdenum phases supported on CNT. Whereas, sulfiding method II results in only partial reduction and partial sulfidation of molybdenum species irrespective of which kind of support is studied.

According to the catalytic HDS measurements it is concluded that carbon nanotube supported CoMo catalysts are of higher HDS activity and selectivity than CoMo/γ-Al_2O_3 catalyst. Co/Mo atomic ratio has great influence on both HDS activity and selectivity, and CoMo-0.7/CNT catalyst is the most active one, while CoMo-0.35/CNT catalyst shows the highest selectivity.

Acknowledgements

The authors wish to thank the Nano-material Research Center of Tsinghua University, who supplied us with different kinds of carbon nanotubes.

References

1 Damyanova, S.; Petrov, L.; Grange, P. *Appl. Catal. A*: *General* **2003**, *239*, 241.
2 Catttaneo, R.; Weber, T.; Shido, T.; Prins, R. *J. Catal.* **2000**, *191*, 225.
3 Damyanova, S.; Spojakina, A. *Catal. Lett.* **1993**, *51*, 465.
4 Vrinat, M.; Hamou, D.; Breysse, M.; Durand, D.; Courieres, T. *Catal. Today* **1994**, *20*, 273.
5 Damyanova, S.; Spojakina, A.; Jiratova, K. *Appl. Catal. A*: *General* **1995**, *125*, 257.
6 Feng, L.; Li, X.; Dadyburjor, D. B. *J. Catal*. **2000**, *190*, 1.
7 Li, Z. R.; Fu, Y. L.; Bao, J.; Jiang, M.; Hu, T.; Liu, T.; Xia, Y. N. *Appl. Catal. A*: G*eneral* **2001**, *220*, 21.
8 Juentgen, H. *Fuel* **1986**, *65*, 1436.
9 Wivel, C.; Clausen, R.; Clausen, B. S.; Morup, S.; Topsoe, H. *J. Catal*. **1981**, *146*, 375.
10 Pan, W. H.; Leonowicz, M. E.; Stiefel, E. I. *Inorg. Chem.* **1983**, *22*, 672.
11 Karakonstantis, L.; Matralis, H.; Kordulis, C.; Lycourghiotis, A. *J. Catal*. **1996**, *162*, 306.
12 Shimada, H.; Sato, T.; Yoshimura, Y.; Hiraishi, J.; Nishijima, A. *J. Catal.* **1988**, *110*, 275.
13 Paterson, T. A.; Carver, J. C.; Leyden, D. E.; Hercules, D. M. *J. Phys. Chem.* **1976**, *80*, 1702.
14 Weber, T. H.; Muijsers, J. C.; Niemantsverdriet, J. W. *J. Phys. Chem.* **1995**, *99*, 9194.
15 Weber, T. H.; Muijsers, J. C.; Van Wolput, J. H. M. C.; Niemantsverdriet, J. W. *J. Phys. Chem.* **1996,** *100*, 14144.
16 Muijsers, J. C.; Weber, T.; Van Hardeveld, R. M.; Zandbergen, H. W.; Niemantsverdriet, J. *J. Catal.* **1995**, *157*, 698.
17 Li, C. P.; Hercules, D. M. *J. Phys. Chem.* **1984**, *88*, 456.
18 Harris, S.; Chianelli, R. R. *J. Catal*. **1986**, *98*, 17.
19 Layuritsen, J. V.; Helveg, S.; Laegssgaard, E.; Stensgaard, I.; Clausen, B. S.; Topsoe, H.; Besenbacher, F. *J. Catal.* **2001**, *197*, 1.
20 Venezia, A. M.; La Parola, V.; Deganello, G.; Cauzzi, D.; Leonardi, G.; Predieri, G. *Appl. Catal. A*: *General* **2002**, *229*, 261.

(E0311196 ZHAO, X. J.)